Atmos. Meas. Tech., 6, 495–509, 2013
www.atmos-meas-tech.net/6/495/2013/
doi:10.5194/amt-6-495-2013

Atmospheric Measurement Techniques
Open Access

Retrieval and satellite intercomparison of O_3 measurements from ground-based FTIR Spectrometer at Equatorial Station: Addis Ababa, Ethiopia

S. Takele Kenea[1], G. Mengistu Tsidu[1], T. Blumenstock[2], F. Hase[2], T. von Clarmann[2], and G. P. Stiller[2]

[1]Department of Physics, Addis Ababa University, P.O. Box 1176, Addis Ababa, Ethiopia
[2]Institute for Meteorology and Climate Research (IMK-ASF), Karlsruhe Institute of Technology (KIT), Karlsruhe, Germany

Correspondence to: S. Takele Kenea (samueltake@yahoo.ca)

Received: 27 July 2012 – Published in Atmos. Meas. Tech. Discuss.: 18 September 2012
Revised: 6 December 2012 – Accepted: 4 February 2013 – Published: 28 February 2013

Abstract. Since May 2009, high-resolution Fourier Transform Infrared (FTIR) solar absorption spectra have been recorded at Addis Ababa (9.01° N latitude, 38.76° E longitude, 2443 m altitude above sea level), Ethiopia. The vertical profiles and total column amounts of ozone (O_3) are deduced from the spectra by using the retrieval code PROFFIT (V9.5) and regularly determined instrumental line shape (ILS). A detailed error analysis of the O_3 retrieval is performed. Averaging kernels of the target gas shows that the major contribution to the retrieved information comes from the measurement. The degrees of freedom for signals is found to be 2.1 on average for the retrieval of O_3 from the observed FTIR spectra. The ozone Volume Mixing Ratio (VMR) profiles and column amounts retrieved from FTIR spectra are compared with the coincident satellite observations of Microwave Limb Sounding (MLS), Michelson Interferometer for Passive Atmospheric Sounding (MIPAS), Tropospheric Emission Spectrometer (TES), Ozone Monitoring Instrument (OMI), Atmospheric Infrared Sounding (AIRS) and Global Ozone Monitoring Experiment (GOME-2) instruments. The mean relative differences in ozone profiles of FTIR from MLS and MIPAS are generally lower than 15 % within the altitude range of 27 to 36 km, whereas difference from TES is lower than 1 %. Comparisons of measurements of column amounts from the satellite and the ground-based FTIR show very good agreement as exhibited by relative differences within +0.2 % to +2.8 % for FTIR versus MLS and GOME-2; and −0.9 to −9.0 % for FTIR versus OMI, TES and AIRS. The corresponding standard deviations are within 2.0 to 2.8 % for FTIR versus MLS and GOME-2 comparisons whereas that of FTIR versus OMI, TES and AIRS are within 3.5 to 7.3 %. Thus, the retrieved O_3 VMR and column amounts from a tropical site, Addis Ababa, is found to exhibit very good agreement with all coincident satellite observations over an approximate 3-yr period.

1 Introduction

The study of atmospheric trace gases has a great role to play in terms of global climate change and atmospheric chemistry. The increase in population growth, accompanied by industrial development and deforestation, have altered the tropical environment. The impact of these changes on atmospheric composition and climate are not fully known due to poor understanding of the physical and chemical processes that govern tropical atmosphere (Petersen, 2009, and references therein). The previous studies show that no significant ozone loss is observed over the tropical stratosphere (Fishman et al., 2005, and references therein); however, recent study shows that O_3 rich airmass can be injected into lower latitudes all the way to equatorial Africa episodically (Mengistu Tsidu and Ture, 2013). Therefore, it is very important to get a clear understanding about this region because this layer also determines the concentration of many short-lived species that are entering into the stratosphere.

Ozone is the most important trace gas, which exists in its largest relative abundance in the stratosphere, between ∼ 15 and 50 km altitude. O_3 absorbs solar ultraviolet (UV) radiation with wavelengths between 200 and 300 nm, shielding

the surface of the Earth from this harmful radiation. The main source of ozone is photolysis reaction. However, O_3 is also destroyed through a number of chemical reactions with other stratospheric trace gases. Ozone in the troposphere is also an important greenhouse gas. Tropospheric ozone is formed through a photochemical process from the natural and anthropogenic emissions.

The tropical NDACC (Network for the Detection of Atmospheric Composition Change) stations at which FTIR measurements are performed are Mauna Loa (19.54° N, 155.6° W) (Rinsland et al., 1988) and Paramaribo (5.8° N, 55.2° W) (Petersen et al., 2008, 2010). Our measurement, Addis Ababa (9.01° N latitude, 38.76° E longitude, 2443 m altitude above sea level), is also located in the tropics. It is the first high resolution FTIR spectrometer on the African continent. The FTIR at Addis Ababa is planned to be part of the NDACC network that has been monitoring long-term atmospheric composition changes. In this study, intercomparisons of vertical profiles and column amounts retrieved from solar spectra observed by Fourier Transform Spectrometer at this site and satellite measurements in different observing modes are made. The observed differences between observations from ground-based FTIR and satellites are investigated based on a full error characterisation analysis.

The paper is structured as follows: Sect. 2 introduces the measurement site and the FTIR spectrometer. Section 3 provides discussion of spectral analysis. Section 4 provides a short description of satellite measurement techniques and this is followed by the detailed intercomparison of the satellite measurements in Sect. 5. Finally, conclusions are given in Sect. 6.

2 Measurement site and instrumentation

2.1 Measurement site

Addis Ababa is located at 9.01° N latitude, 38.76° E longitude, 2443 m altitude above sea level, which is in the equatorial region. It is relatively dry due to its topography, making it robust for monitoring trace gas species in the tropics since interference of tropospheric water vapour absorption lines is of minor relevance. Moreover, the typical tropopause height for tropical regions is between 16 to 18 km, and the corresponding temperature is about 200 K. The tropical tropopause region is the transition layer between the dynamical control of the vertical mass flux by tropospheric convection and by the stratospheric Brewer-Dobson circulation (Holton, 2004; Jacobson, 2005). Thus, the site is highly affected by tropical dynamics allowing us to understand processes that modulate tropical dynamics from the observed variation in the measurement of atmospheric trace gases. Ethiopia experiences generally southwesterly moisture laden air from South Atlantic and Indian Ocean during northern summer, whereas it is under the influence of dry continental northeasterly winds during northern winter. The detailed climatology of the region is described by Mengistu Tsidu (2012) and references therein. Therefore, this FTIR site is also ideal to observe seasonal variation as ITCZ migrates north-south with season across the site.

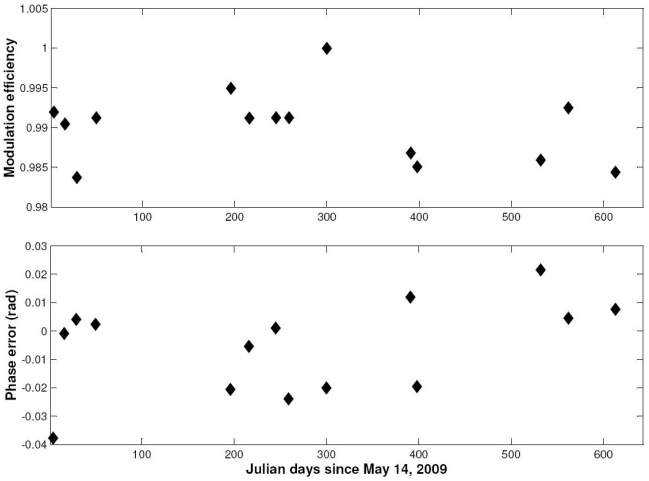

Fig. 1. Evolution of the ILS during the measurement period.

2.2 The FTIR spectrometer and retrieval

The BRUKER interferomenter is based on the IFS-120M model, but upgraded with the new electronics of the model IFS-125M. The FTIR spectrometer has two detectors: mercury–cadmium–telluride (Hg–Cd–Te) and indium antimonide (InSb), which allow coverage of the 600–1500 and 1500–4400 cm^{-1} spectral intervals, respectively. Recently, a new laser source with power supply has been mounted on this interferometer in order to improve the laser signal that reaches the detector to attain stable movement of the optics. Typically, spectral resolution of 0.009 cm^{-1} is applied. FTIR spectrometer makes direct solar absorption measurements throughout the day, under clear sky conditions. The spectra are typically constructed by co-adding up to 10 scans recorded in about 8 min. A very large number of species of atmospheric relevance can be detected owing to its wide spectral coverage. In this paper, O_3 VMR profiles and column amounts are derived from measured spectra using version 9.5 of the retrieval code PROFFIT.

PROFFIT was developed to analyse solar absorption spectra measured with high-resolution ground-based FTIR spectrometers; and it has been compared to other retrieval codes (Hase et al., 2004). Daily pressure and temperature profiles used in the retrievals are taken from the automailer system of Goddard Space Flight Centre. The climatological profiles are based on data from the National Centre for Environment Prediction (NCEP) (http://www.cdc.noaa.gov/data/gridded/data.ncep.reanalysis.html). Spectroscopic data are taken from the High Resolution Transmission data

(HITRAN) 2004 database (Rothman et al., 2005). PROFFIT includes various retrieval options such as scaling of a priori profiles, the Tikhonov-Phillips method (Phillips, 1962; Tikhonov, 1963), or the optimal estimation method (Rodgers, 1976). In this study, Tikhonov-Phillips regularisation method is used during the retrieval.

The retrieved state vector contains the retrieved logarithm of volume mixing ratios of the target gas defined in discrete levels in the atmosphere and retrieved interfering species column amounts, and fitted values for some model parameters. These include the baseline slope and instrumental line shape parameters. The retrieval of O_3 VMR profiles is performed on a logarithmic scale because O_3 concentrations around the tropopause are highly variable. Under these conditions a logarithmic scale inversion is superior to a linear inversion (Hase et al., 2004; Schneider et al., 2006a).

As discussed in Rodgers (2000), the Optimal Estimation Method allows the characterisation of the retrievals, i.e., the vertical resolution of the retrieval, its sensitivity to the a priori information and degree of freedoms for signal (DOFs) are quantitatively described. The retrieved state vector $\hat{\boldsymbol{x}}$ related to the a priori and the true state vectors $\boldsymbol{x}_a$ and $\boldsymbol{x}$, are given by

$$\hat{\boldsymbol{x}} = \boldsymbol{x}_a + \hat{\mathbf{A}}(\boldsymbol{x} - \boldsymbol{x}_a) + \text{ error terms} \quad (1)$$

respectively, where $\hat{\mathbf{A}}$ is averaging kernel matrix. The actual averaging kernels matrix depends on several parameters including the solar zenith angle, the spectral resolution and signal-to-noise ratio, the choice of retrieval spectral microwindows, and the a priori covariance matrix $\mathbf{S}_a$. The elements of the averaging kernel for a given altitude give the sensitivity of the retrieved profile at that altitude to the real profile at each altitude, and its full width at half maximum is a measure of the vertical resolution of the retrieval at that altitude (Vigouroux et al., 2007). Error estimation analysis is based on the analytical method suggested by Rodgers (2000):

$$\hat{\boldsymbol{x}} - \boldsymbol{x} = (\hat{\mathbf{A}} - \mathbf{I})(\boldsymbol{x} - \boldsymbol{x}_a) + \hat{\mathbf{G}}\hat{\mathbf{K}_p}(p - \hat{p}) + \hat{\mathbf{G}}\epsilon \quad (2)$$

where $\hat{p}$, p are the estimated and real model parameters, respectively, $\hat{\mathbf{G}}$ is the gain matrix, $\hat{\mathbf{K}}_p$ is the model parameter sensitivity matrix and ϵ represents noise. The first term in Eq. (1) represents the smoothing error. The second term stands for the estimated error due to uncertainties in input parameters, such as instrumental parameters or spectroscopic data, the $p - \hat{p}$ is only valid for fully correlated perturbations of p (assuming that p is a vector). In addition, the third term represents the error due to the measurements noise.

The full width at half maximum of absorbtion lines of stratospheric gases and of ILS have similar magnitudes. Therefore, regular cell measurements using the LINEFIT software (Hase et al., 1999) were used to derive the instrument line shape (ILS) of the spectrometer so that it could be used in the retrievals. Using the globar as a source of IR radiation, up to 100 scans are co-added to get spectra with and without the presence of an HBr cell placed in the parallel beam of a radiation source. The LINEFIT software was used to compute ILS by comparing the measured line shape with the theoretical one. We obtained modulation efficiency and phase error during the measurement period May 2009 to February 2011 as in Fig. 1. Figure 1 illustrates that the modulation efficiency remains nearly constant with minor fluctuation over a range of 98–100 %. The phase error is also confined to ± 0.02 rad. Therefore, there was an excellent instrumental alignment for a period of more than 2 yr considered in this study. However, we found that at the beginning of the observation period, there were low ADC (Analog to Digital Convertor) counts which we are unable to pinpoint as to its cause from our metadata. Hence, the results for May and June 2009 are excluded from the intercomparison.

3 Information content and error analysis

The information on the retrieval of vertical distribution and column amounts of O_3 from ground-based high resolution FTIR spectra are discussed in the following. Information on the vertical distribution of O_3 is obtained from the spectra because the shape of the absorption features are influenced by pressure broadening. While the line centres provide information about the higher altitudes of the distribution, the wings of a line provide information about the lower altitudes. Therefore, the information content of the retrieval will strongly depend on the choice of the absorption lines. The other important requirement that has been taken into consideration to perform this task successfully is a good knowledge of pressure and temperature profiles. Sensitivity of retrieval as function of altitude and error budget have been analysed thoroughly to ensure information coming from the measurement overweighs that from the a priori as much as possible as a trade off between getting a smoothed profile and enhancing information from measurement. Spectral microwindows found to be best in this sense for O_3 retrievals are those near 3041, 3045 and 3051 cm^{-1}, for the InSb measurements. These spectral regions have high sensitivity in the stratosphere and negligible sensitivity in the troposphere. The micro-windows near 1000 cm^{-1} are best suited for the retrieval of ozone since they have highest sensitivity to both the stratosphere and troposphere which has been reported in different papers (Barret et al., 2002, 2003; Schneider et al., 2008; Lindenmaier et al., 2010) for the MCT measurement, however, in our case, we have far more InSb measurements than MCT measurements. Moreover, the few observations that exist in MCT detection range are of bad quality due to problems with KBr beam splitter. In this analysis, therefore, we considered six micro-windows in the spectral region between 3039.37 to 3051.90 cm^{-1} which are determined from ALFIP software (Notholt et al., 2004).

The major absorption lines of interfering gases in these spectral micro-windows are H_2O and CH_4. There are also minor interferences from CH_3D, CH_3Cl, C_2H_4 and solar lines. Figure 2 (first and third row panels) show example of

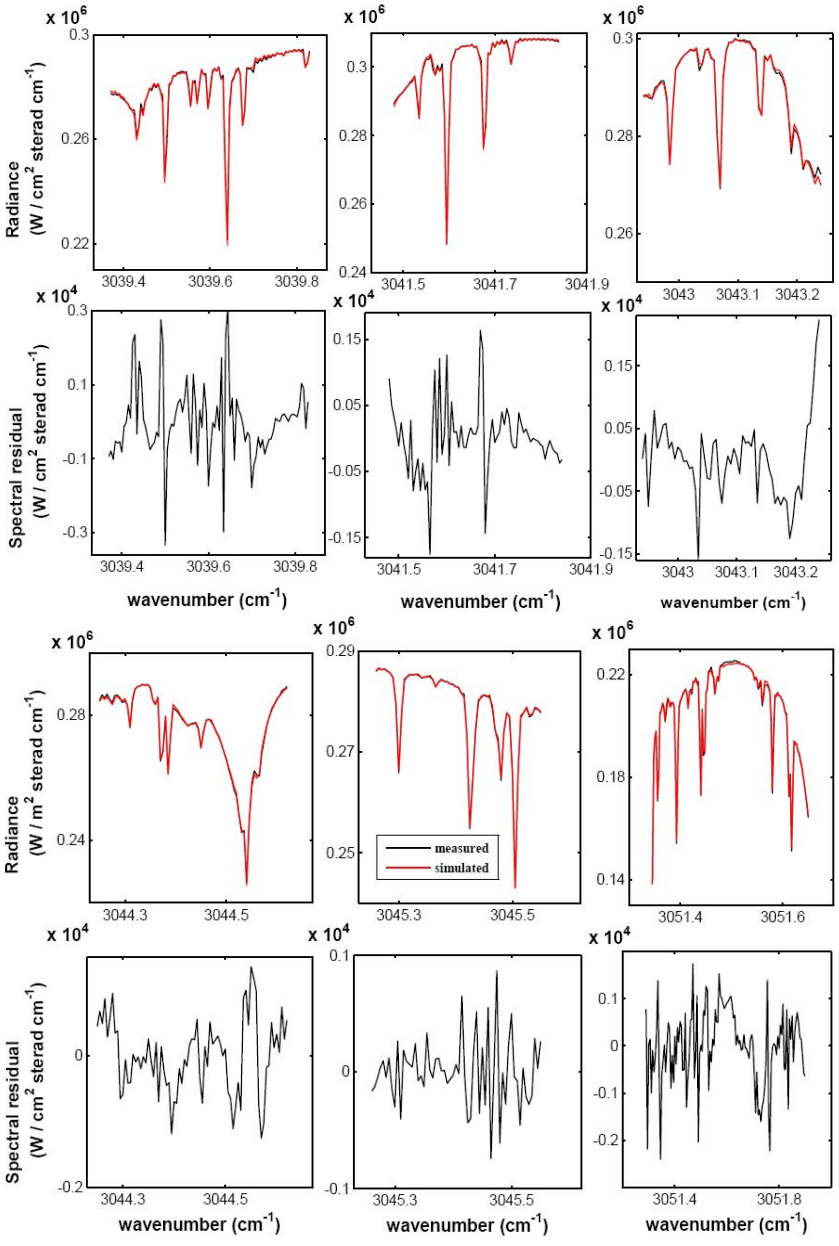

Fig. 2. O_3 – The top and the third panels show the measured spectrum (black line) and simulated spectrum (red line); and the second and the bottom panels show corresponding spectral residuals on 27 May 2010 for different spectral micro-windows.

measured spectra (black line) and the corresponding simulated spectra (red), as well as the residual spectra (second and fourth row panels) in each micro-windows for one of the measurements taken on 27 May 2010. The residual spectra span a range of a maximum of +3 % to −3.2 %.

Figure 3 shows averaging kernels matrix (left panel) while its rows shown (right panel) depict the same information, but more clearly the response in two different altitude ranges. For ideal retrieval for which the ozone profile is purely determined by measurement, the averaging kernel will be unit matrix. The full width at half maximum of the rows of the averaging kernel gives the vertical resolution, which is in the order of 9–15 km for the retrieved O_3 in this study. The sensitivity of the spectra to perturbation in VMR at each height is shown by well defined and sharp rows of the averaging kernel based on the a priori result. This means that the retrievals of O_3 are mainly sensitive in the altitude range of 16 to 40 km as indicated in Fig. 3. Furthermore, the trace of the averaging kernel matrix, the so called degree of freedom for signals, provides another useful measure of retrieval quality of target species. The independent pieces of information retrieved from the observed spectra in the O_3 spectral micro-windows

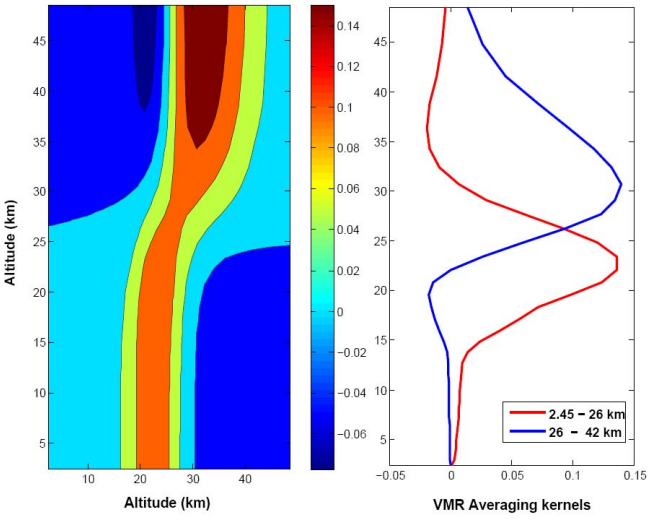

Fig. 3. The left panels show O_3 averaging kernels matrix and the right panels depict rows of averaging kernels (ppmv ppmv^{-1}) for two altitude ranges shown in the legend for retrieval based on FTIR observation taken on 27 May 2010.

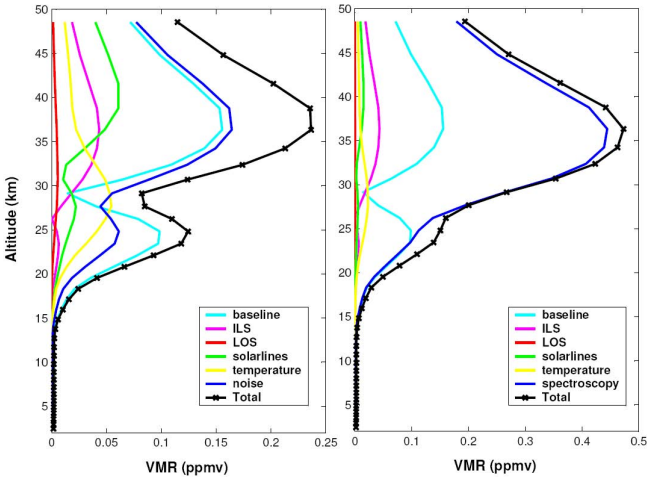

Fig. 4. Error budget of O_3 retrieval from solar spectra taken by FTIR. Left: estimated uncertainty profiles for statistical error. Right: systematic error contributions.

under the given retrieval strategy contain about 2.1 degree of freedom for signals (dofs). This provides 2 independent layers, which approximately covers the altitude range of 2.5 to 26 km and 26 to 40 km as marked by basically two dominant peaks of rows of averaging kernel in Fig. 3 (right panel). The value of dofs obtained in this study is relatively small as compared to the values reported in the literatures (e.g. Lindenmaier et al., 2010; Schneider et al., 2005a). Different degrees of freedom for signal can be obtained due to application of different micro-windows with different spectral resolution and the choice of a priori covariance matrix. Wunch et al. (2007) reported 2.1–2.4 dofs for ozone retrieval by applying micro-windows near 2775 and 3040 cm^{-1} with different spectral resolution during instruments intercomparison campaign at University of Toronto. The ozone peak altitude over tropics as found in this measurement is around 32 km. This altitude is higher than the corresponding ozone peak altitude at higher latitudes which are in the order 25–28 km in most cases. This difference in ozone peak altitude could be one of a possibility for small degree of freedom since profile information from measurement is a function of strength of pressure broadening.

The contribution of different sources of errors that contributed to the quality of measurement of the target gas is displayed in Fig. 4. Figure 4 shows the statistical error (left panel) and systematic error (right panel) profiles for a typical O_3 retrieval. The major sources of errors quantified in this study include temperature, measurement noise, instrumental line shape, solar lines, line of sight, zero baseline offset and spectroscopy. One can note from Fig. 4 that the main systematic error source is the uncertainty of spectroscopic parameters, whereas the major statistical error source is measurement noise. The contribution of error from uncertainty in solar lines and line of sight to O_3 profile retrieval is the lowest. The maximum estimated systematic and statistical error budget reach up to 0.6 ppmv around 31 km and 0.2 ppmv at 35 km, respectively. The main systematic error sources for partial columns for the O_3 retrieval from ground-based FTIR are O_3 line intensities and air broadening coefficients (Barret et al., 2002, 2003) which could partly explain the observed biases. Whenever averages are calculated on the basis of log retrievals, this might be causing bias (Funke and von Clarmann, 2012) for trace species with large vertical gradient. Though, the extent of such impact on ozone has not yet fully characterised, there is a possibility that it might have some influences. By adding up systematic and statistical error sources for a given altitude and then integrating it along the error patterns (Rodgers, 2000), we found the total systematic and random error of O_3 total columns to be 2.1 % and 0.8 %, respectively. The total systematic error on the total columns is in good agreement with those found in Viatte et al. (2011), and references therein. But the total random error for the total columns estimated in this study is 0.3 % higher than those reported by Viatte et al. (2011), which might be linked with a difference in spectral resolution.

4 Satellite measurements

4.1 Microwave Limb Sounder (MLS)

The Earth Observing System (EOS) Microwave Limb Sounder (MLS) is one of four instruments on the NASA EOS Aura satellite (Schoeberl et al., 2006), launched on 15 July 2004 into a near polar sun-synchronous orbit at an altitude of 705 km, with ascending equatorial crossing time of 13:45 (local time). The Aura-MLS instrument, calibration

Table 1. Summary of the characteristics of the instruments and measurement systems of O_3 addressed in this study.

Instruments	FTIR	MLS	MIPAS	TES	OMI	AIRS	GOME-2
Platform	Ground-based	Satellite	Satellite	Satellite	Satellite	Satellite	Satellite
Observation geometry	upward	limb	limb	nadir	nadir	nadir	nadir
Observation mode	absorption	emission	emission	emission	backscattered	emission	backscattered
Vertical resolution (km)	$\sim$ 9–15	3–4	3.5–5	$\sim$ 6	3–5	greater than $\sim$ 6	3–5
Spectral resolution	0.009 cm^{-1}	6–96 MHz	0.0625 cm^{-1}	0.1 cm^{-1}	0.42–0.63 nm	0.5–2 cm^{-1}	$\sim$ 0.24 nm
Spectral domain	600–4400 cm^{-1}	$\sim$ 80 000 cm^{-1} ($\sim$ 240 GHz)	685 2410 cm^{-1}	650–2250 cm^{-1}	270–330 nm	650–2700 cm^{-1}	325–335 nm

and performance for the different channels are described by Jarnot et al. (2006). In this work, we have used version 2.2 of MLS O_3 dataset for comparison to FTIR result. The MLS version 2.2 O_3 profiles is the standard ozone product retrieved from radiance measurements near 240 GHz. It has been extensively characterised and validated (Froidevaux et al., 2008; Jiang et al., 2007; Livesey et al., 2008). More details regarding the MLS experiment and O_3 data screening are provided in the above references in detail and at http://mls.jpl.nasa.gov/data/datadocs.php.

4.2 Michelson Interferometer for Passive Atmospheric Sounding (MIPAS)

The MIPAS instrument is a high-resolution atmospheric limb sounder aboard ESA's ENVISAT launched in March 2002 and operating in a sun-synchroneous orbit. It aims at global and simultaneous measurements of the chemical composition of the middle atmosphere and upper troposphere. The pointing system allows MIPAS to observe atmospheric parameters in a maximum altitude range of 5–160 km with a vertical spacing of 1–8 km depending on the altitude and the measurement mode (Fischer et al., 2008). In this study, we have used the reduced spectral resolution (Institute for Meteorology and Climate Research) IMK/IAA MIPAS ozone data product V5R_O3_220 (von Clarmann et al., 2009) for comparison purpose. The first validation of reduced resolution IMK/IAA ozone data was reported by Stiller et al. (2012).

4.3 Tropospheric Emission Spectrometer (TES)

The Tropospheric Emission Spectrometer (TES) launched into sun-synchronous orbit on aboard Aura, the third of NASAs Earth Observing System (EOS) spacecraft, on 15 July 2004. TES is an infrared high spectral resolution (0.1 cm^{-1} after Norton-Beer medium apodisation in nadir) (Beer et al., 2001) spectrometer. TES Level 3 O_3 data have been used for comparison in this work. TES ozone data have been evaluated by comparison to ozonesondes (e.g. Nassar et al., 2008; Worden et al., 2007), aircraft data (e.g. Richards et al., 2008), and ozone measured by other satellite instruments (e.g. Zhang et al., 2010).

4.4 Ozone Monitoring Instrument (OMI)

Ozone Monitoring Instrument (OMI), is one of the four instruments on EOS-Aura. OMI is a Dutch-Finnish built nadir-viewing UV/visible instrument. It has been measuring backscattered radiances in three channels covering the 264–504 nm wavelength range (UV-1: 264–311 nm, UV-2: 307–383 nm, visible: 349–504 nm) at spectral resolutions of 0.42–0.63 nm (Levelt et al., 2006). In this study, we have used OMI level 3-D ozone total column amounts for comparisons. OMI total ozone column measurements have been evaluated by comparison to Brewer and Dobson spectrophotometer ground-based observations (Balis et al., 2007). More details about the instrument and its scientific objectives can be found in the Science Requirements Document for OMI-EOS (http://aura.gsfc.nasa.gov/).

4.5 Atmospheric Infrared Sounding (AIRS)

The Atmospheric Infrared Sounder (AIRS) instrument is one of several instruments onboard the Earth Observing System (EOS) Aqua spacecraft launched 4 May 2002. The AIRS instrument has been operating to scan the Earth's atmosphere in nadir viewing. AIRS daily Level 3 version 5 O_3 standard products are considered for comparison and its spatial resolution is 1° latitude and 1° longitude. Further details about

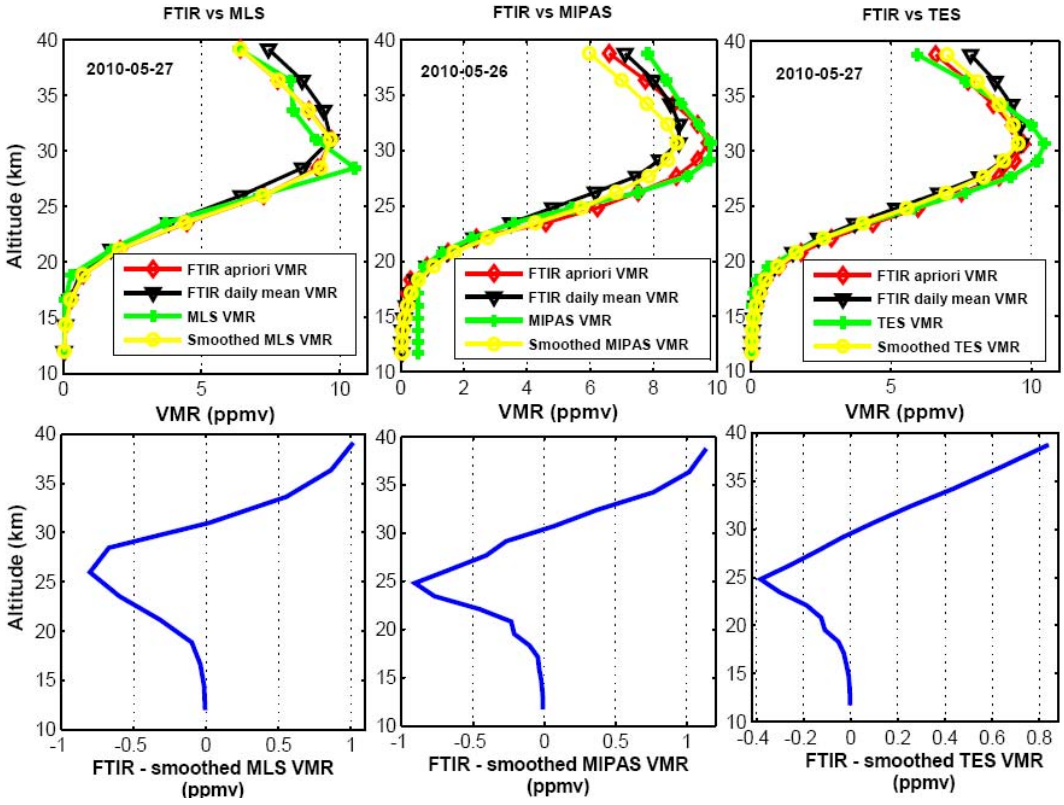

Fig. 5. Top: Comparisons of O_3 VMR profiles on 26 and 27 May 2010. FTIR a priori (red with diamond symbol) and FTIR daily mean (black with triangle symbol) are shown in top panels, MLS smoothed (yellow with circle) and MLS (green with plus sign symbol) (left top panel), MIPAS smoothed (yellow with circle) and MIPAS (green with plus sign symbol) (middle top panel) and TES smoothed (yellow with circle) and TES (green with plus sign symbol) (right top panel). Bottom: absolute differences (in ppmv) between FTIR and smoothed MLS (left bottom panel), FTIR and smoothed MIPAS (middle bottom panel) and FTIR and smoothed TES (right bottom panel).

the overview of AIRS instruments can be found in Young-In Won (2008) and at http://disc.gsfc.nasa.gov.

4.6 Global Ozone Monitoring Experiment (GOME-2)

The Global Ozone Monitoring Experiment (GOME-2) aboard MetOp-A is a scanning spectrometer that captures light reflected from the Earth's surface and backscattered by the atmosphere. The spectrometer splits the light into its spectral components covering the UV/VIS region from 240 nm to 790 nm at a resolution of 0.2 nm to 0.4 nm. Error analysis indicates an accuracy and precision of O_3 total columns of 3.6–4.3 % and 2.4–3.3 %, respectively, when the solar zenith angle is below 80° (Van Roozendael et al., 2004). Total ozone columns derived from this algorithm have been validated using ground-based networks (Balis et al., 2007, 2008). Further details of the document can be obtained from http://wdc.dlr.de/sensors/ gome2. In this paper, we have used O_3 columns from GOME-2 Level 3 data.

5 Comparison of FTIR O_3 VMR profiles and column amounts with MLS, MIPAS, TES, OMI, AIRS and GOME-2 observations

5.1 Comparison methodology

The closest satellite measurements (on the same day as the ground-based FTIR measurements) within ±2 degrees of latitude and ±10 degrees of longitude are selected for intercomparison. The more stringent latitudinal criterion has proven to be a good choice for all comparisons, since latitudinal variations are, in general, more pronounced than longitudinal ones. These criteria yielded 67, 14, 6, 60, 57 and 42 days of coincident measurements between FTIR and MLS, MIPAS, TES, OMI, AIRS and GOME-2, respectively. All the satellite data (MLS, MIPAS, TES, OMI, AIRS and GOME-2) used in the following comparisons have considerably better vertical resolution than ground-based FTIR profiles due to observation geometry, spectral windows and measurement techniques. The vertical resolution of satellite measurements of profiles are, therefore, degraded to facilitate a comparison between the two sets of profiles. Therefore, the satellite

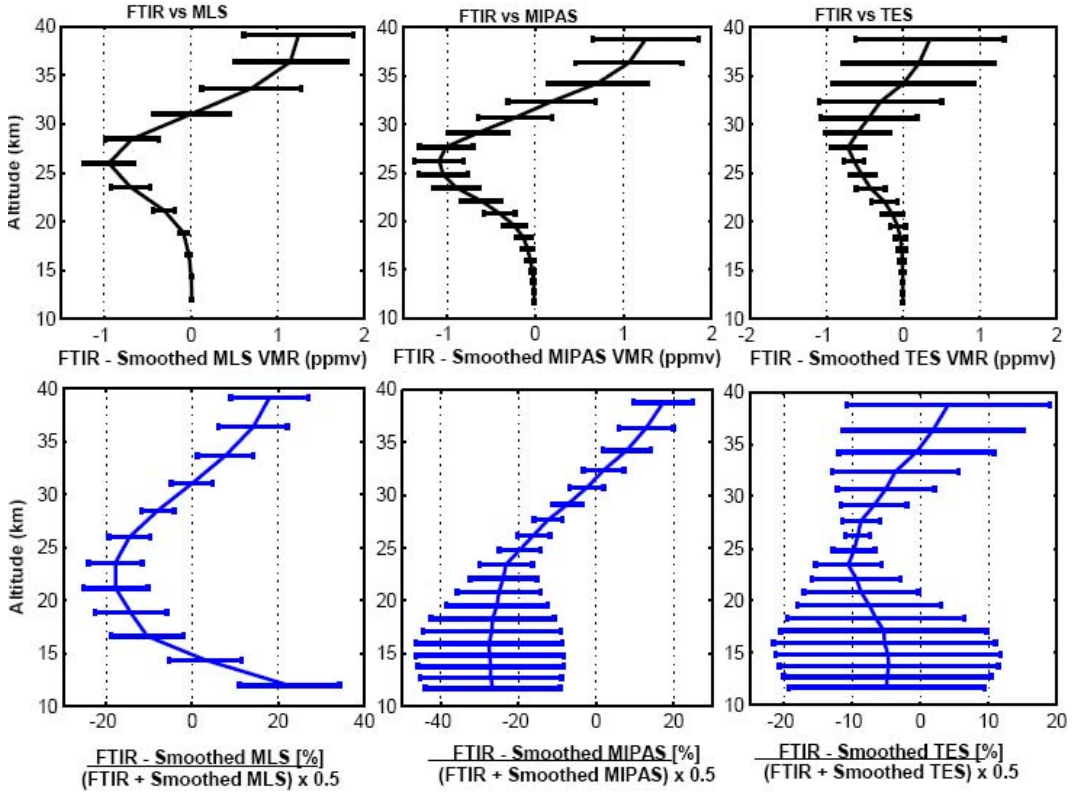

Fig. 6. Statistics for intercomparison of O_3 VMR profiles between FTIR and satellites instruments (MLS, MIPAS and TES). Top: mean of the differences and its standard deviation (shown as error bar) for FTIR-MLS (left), FTIR-MIPAS (middle) and FTIR-TES (right). Bottom: the same as top panels but for relative differences.

measurement profiles are smoothed using the averaging kernels calculated during the ground-based FTIR retrieval process as proposed by Rodgers and Connor (2003). The techniques described have been validated against other measurements of O_3 at different locations (e.g. Hoogen et al., 1999; Lucke et al., 1999; Schneider, 2002; Mengistu Tsidu, 2005).

The equation relating FTIR and satellites can be given by

$$\hat{\boldsymbol{x}}_{\mathrm{s}} = \boldsymbol{x}_{\mathrm{a}} + \hat{\mathbf{A}}_{\mathrm{FTIR}}(\boldsymbol{x}_{\mathrm{Sat}} - \boldsymbol{x}_{\mathrm{a}}) \tag{3}$$

where $\boldsymbol{x}_{\mathrm{Sat}}$ is the original satellite measurement profile, $\hat{\boldsymbol{x}}_{\mathrm{s}}$ is the smoothed profile, and $\boldsymbol{x}_{\mathrm{a}}$ and $\hat{\mathbf{A}}_{\mathrm{FTIR}}$ are the a priori profile and the averaging kernel matrix of the ground-based FTIR instrument, respectively. To calculate the profile of the mean absolute difference, the differences are calculated for each pair of profiles at each altitude, and then averaged at altitude z as

$$\triangle_{\mathrm{abs}}(z) = \frac{1}{N(z)} \sum_{i=1}^{N(z)} [\mathrm{FTIR}_i(z) - \mathrm{Sat}_i(z)] \tag{4}$$

where $N(z)$ is the number of coincidences at z, $\mathrm{FTIR}_i(z)$ is the FTIR VMR at z and the corresponding $\mathrm{Sat}_i(z)$ VMR for the validation instrument. Note that the term absolute, as used in this work, refers to differences between the compared values, in VMR as opposed to percentage or relative differences, in other words: absolute differences can be negative. To calculate the profile of the mean relative difference, as a percentage, we used

$$\triangle_{\mathrm{rel}}(z) = 100(\%) \times \frac{1}{N(z)} \sum_{i=1}^{N(z)} \frac{[\mathrm{FTIR}_i(z) - \mathrm{Sat}_i(z)]}{[\mathrm{FTIR}_i(z) + \mathrm{Sat}_i(z)]/2} \tag{5}$$

In some cases, there seems to be a discrepancy between the apparent differences given by the sign of the mean absolute and mean relative differences. This arises due to the fact that the mean relative differences are not calculated from the mean VMR profiles, but from each pair of coincident profiles (Eq. 4). Thus, the mean relative differences can become negative, even though the mean absolute differences are positive. A comparison of the total column amounts between FTIR and its correlative measurements has been done by employing the FTIR averaging kernels for smoothing. The relative differences of the total column amounts between FTIR and its correlative measurement from MLS, TES, OMI, AIRS and GOME-2 instrument for coinciding dates can be defined as

$$\text{Rel. diff.}(\%) = \left(\frac{[\mathrm{FTIR}_i(\mathrm{TC}) - \mathrm{Sat}_i(\mathrm{TC})]}{[\mathrm{FTIR}_i(\mathrm{TC}) + \mathrm{Sat}_i(\mathrm{TC})]/2}\right) \times 100 \tag{6}$$

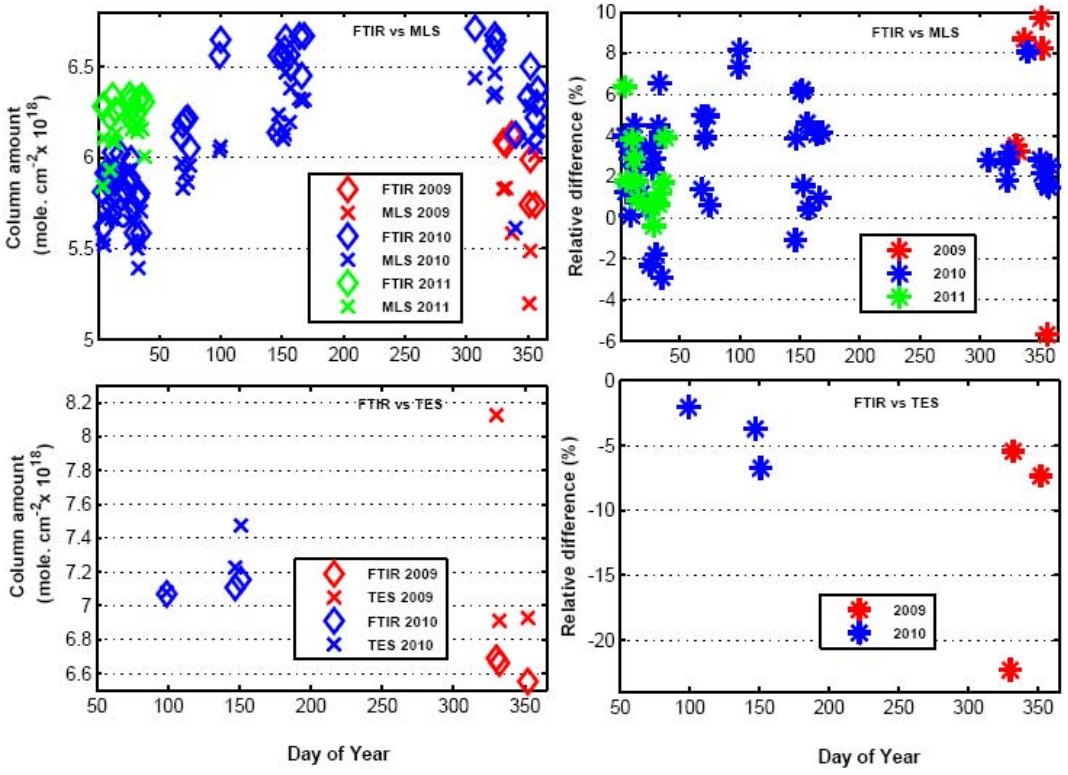

Fig. 7. Top-left panel shows column amounts of O_3 for FTIR (open diamonds) and the corresponding MLS measurements (cross) for different observations years (in colour), bottom-left panel shows column amounts between FTIR (open diamonds) and TES (cross). Right panels depict the relative differences between FTIR and MLS (right top panel), FTIR and TES (right bottom panel).

Table 2. Summary of the comparison between O_3 columns amount derived from FTIR and from various satellites data (MLS, TES, OMI, AIRS and GOME-2) over Addis Ababa. *N* represents number of coincidences.

Comparison of FTIR with	*N*	Mean Relative Difference (%)
MLS	67	2.8 ± 2.8
TES	6	-7.9 ± 7.3
OMI	60	-0.9 ± 3.5
AIRS	57	-9.0 ± 5.7
GOME-2	42	0.2 ± 2.0

where "TC" represents total column amount and Sat_i(TC) refers to correlative satellite measurement. Moreover, data are screened to reject either the whole profile or identified low-quality measurements at some altitudes from each instrument according to the recommendations provided by each calibration and processing team.

5.2 Intercomparison of VMR profiles

Figure 5 (left top panel) shows an example of a comparison of O_3 profiles between ground-based FTIR and MLS version 2.2 on 27 May 2010. Figure 5 (left bottom panel) depicts the absolute difference between FTIR and smoothed MLS profiles of O_3. FTIR O_3 VMR exceeds slightly MLS O_3 VMR above 31 km altitude. Figure 6 (left top and bottom panels) shows the statistical relationship for all 67 coincidences for O_3 VMR. The left-top panel shows the mean absolute differences (ppmv) and the left-bottom panel is mean relative differences (%). Error bars represent the standard deviation. The mean relative differences are within −18 to +20 % above 16.6 km.

The comparison of ozone profiles derived from the FTIR and MIPAS in the altitude between 11.7 and 40 km have been analysed. Middle panels of Fig. 5 show that the comparison of O_3 profiles from ground-based FTIR with MIPAS IMK/IAA ozone profiles (version V5R_O3_220) on 26 May 2010. Figure 5 (Middle bottom panel) depicts the absolute difference between FTIR and smoothed MIPAS profiles of O_3. FTIR O_3 VMRs are slightly larger than MIPAS measurements above 35 km. The magnitude of the largest absolute difference is 1.7 ppmv (−20.4 %) around 27.7 km. Figure 6, middle panels, show the statistical relationship for 14 coincident measurements of the two instruments. The mean relative differences are within ±20 % above 23 km.

Steck et al. (2007) compared MIPAS O_3 VMR profiles with ground-based FTIR over different stations and found the

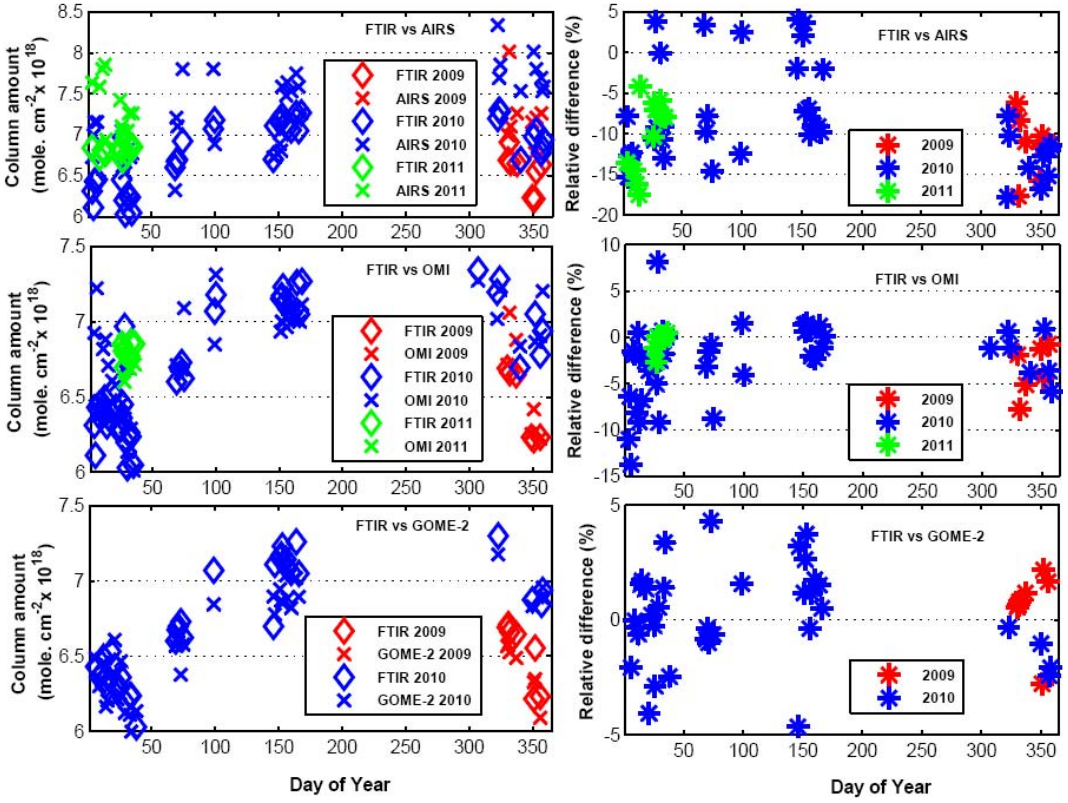

Fig. 8. The same as Fig. 7, but for intercomparison of FTIR with AIRS, OMI and GOME-2 as shown in the figure legend.

mean differences within ±10 % in the middle stratosphere, which is also comparable to the differences found in the comparison of O_3 VMR profiles of FTIR with MIPAS in this study.

Top-right and bottom panels of Fig. 5 show an example of the comparison of O_3 profiles derived from ground-based FTIR with profiles from TES at Addis Ababa on 27 May 2010. The comparison result reveals that TES O_3 VMRs are slightly larger than FTIR measurements above 35 km. The largest absolute difference is about −0.7 ppmv and the corresponding relative discrepancy is about −6 % at the altitude of 27 km. Figure 6 (right panels) show the statistical relationship for 6 coincident measurements for O_3 profiles. The mean relative differences lie between −10.5 to +4.0 % in the altitude range of 11.7–36.3 km where the mean absolute differences are within −0.6 ppmv to +0.3 ppmv. TES ozone data have been evaluated by comparison to ozonesondes (e.g. Nassar et al., 2008; Worden et al., 2007). For example, Nassar et al. (2008) reported differences that exceeds 20 % at low altitudes over tropics.

Inter-comparisons depicted in Figs. 5–6 show differences on the level of agreement between correlative measurements as a function of altitude. There is apparent difference between troposphere and stratosphere presumably due to the difference in the role of dynamics and chemistry. Furthermore, the discrepancy of the result could be partly explained by known contributions to the systematic error budget of the comparison.

5.3 Intercomparison of column amounts

Figure 7 (left top panels) depicts the comparisons of daily time series of O_3 stratospheric columns of FTIR and MLS. The left top panel in Fig. 7 shows the results of FTIR measurements and of collocated MLS data while in the right top panel, the relative difference between them is displayed. As evident from Table 2, a mean relative difference of (2.8 ± 2.8) % reveals that this is statistically significant. In general, FTIR column amounts are about 2.8 % higher than MLS values, which is slightly less than the total uncertainty of FTIR O_3 column amounts of the measurements.

FTIR O_3 total columns are also compared to TES measurements. Figure 7 (bottom panels) displays the comparisons of time series of O_3 total columns of FTIR and TES. On 6 occasions, the mean relative difference of FTIR data is (-7.9 ± 7.3) %. This would suggest that they are in good agreement. We did not compute the correlation coefficient because the sample size is small.

Figure 8 (left top panels) depicts the comparison of O_3 total columns of FTIR and AIRS. The 57 coincident days are found based on the coincidence criteria given in Sect. 5.1. The right top panel shows the relative differences between

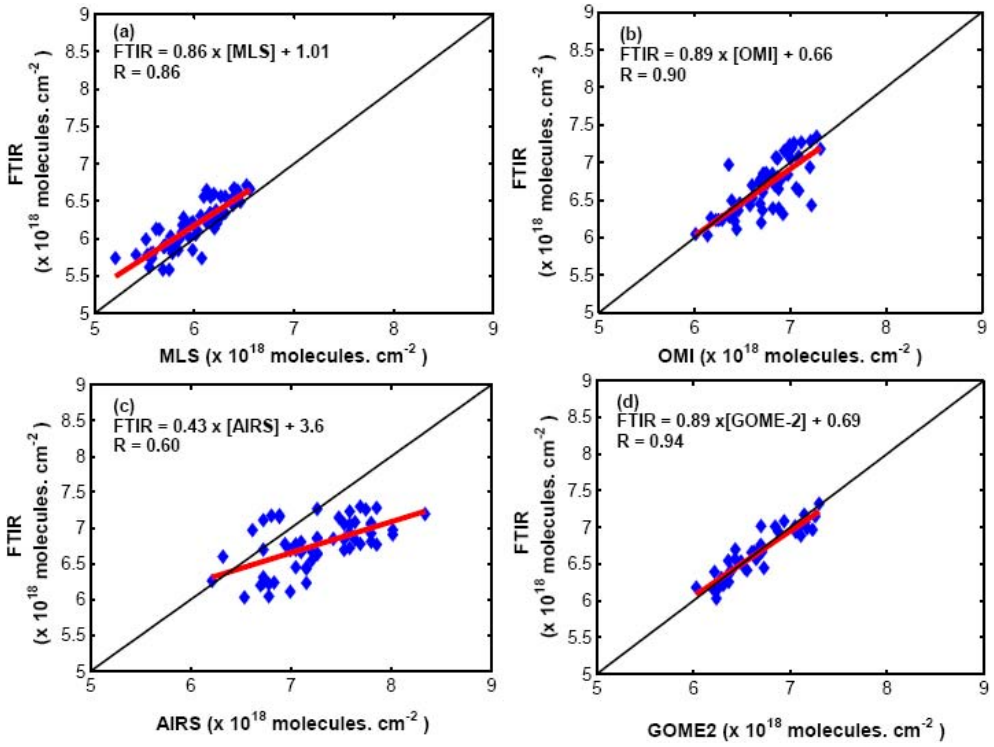

Fig. 9. Scatter plot of columns amount of O_3 measured by ground-based FTIR versus those observed by MLS, OMI, AIRS and GOME-2. In all panels, the red line shows linear fit line of the data pairs that are intercompared. The slope and "R" for the comparisons are also shown in the panels. The black solid line shows the one-to-one line of 100 % correlation.

FTIR and AIRS total columns. The relative differences between the FTIR and AIRS total columns are generally within the range of +5 % to −20 %. This suggests that the absolute difference of the column amount is bounded within $\pm 1.3 \times 10^{18}$ mol cm^{-2}. In general, the mean relative difference is found to be (-9.0 ± 5.7) % (see Table 2).

Figure 8, left middle panel, shows the comparisons of time series of O_3 total columns of FTIR and OMI over Addis Ababa. Based on the coincidence criteria given in Sect. 5.1, 60 coincident days are found. A very good agreement is observed between FTIR and OMI measurements since the overall mean relative difference between them shown in Table 2 is (-0.9 ± 3.5) % which is statistically insignificant. The mean relative difference of our result is slightly higher than the mean relative differences of the previous comparisons between FTIR and OMI made by Viatte et al. (2011). The FTIR measures systematically higher O_3 total columns than the OMI instrument, which may be due to the difference in spectral regions, UV in OMI case and mid-infrared in FTIR case (Viatte et al., 2011, and references therein).

FTIR O_3 column amounts have been compared to GOME-2 measurements as shown in the bottom panels of Fig. 8. Based on the coincidence criteria, 42 coincident days are found. The right lower panel shows the relative difference between FTIR and GOME-2 total column amounts. In general, the mean relative differences between FTIR and GOME-2 total columns are 0.2 ± 2.0 %. This indicates that there is better agreement between FTIR and GOME-2 measurements. The most likely explanations for the differences between the measurements are known bias between the UV and IR spectroscopy. However, the difference is statistically insignificant. The mean relative difference of 1.8 % agrees with the previous comparison study (Viatte et al., 2011).

The comparison of FTIR measurements of O_3 column amounts has been done with different instruments such as Brewer spectrometer (Schneider et al., 2005) with very small differences in contrast to satellite measurements from Improved Limb Atmospheric Spectrometer-II (ILAS-II) (Griesfeller et al., 2006) with the relative differences within 10 to 15 % for vertical VMR profiles. Senten et al. (2008) reported that mean relative differences between ACE-FTS and ground-based FTIR vary between −14 and +12 %, in the middle troposphere ($\sim$ 6 km) up to the stratopause ($\sim$ 47 km) which are similar to the results presented here.

The correlation coefficient between FTIR and MLS column amounts is also depicted in Fig. 9a (left top panel). The correlation coefficient of 0.86 suggests strong relationship between the two datasets. For further understanding of the differences between FTIR and AIRS comparison, we examined the correlation between the instruments. Figure 9, left bottom panel, displays the correlation between FTIR and AIRS column amounts of O_3 for the given coincident data

as characterised by the correlation coefficient of 0.60. Right-top panel of Fig. 9 shows a good correlation of 0.90 between FTIR and OMI data for the coincident periods.

Some of the differences between the FTIR and satellite observations could have arisen from a strong gradient in ozone spatial and temporal variations, even though there is no large difference in space and time for the criteria used to determine coincident measurements. The tropics are well characterised by strong dynamics so that it could contribute to the variation of ozone amount. As reported by Mengistu Tsidu and Ture (2013), there is also strong interaction between tropics and midlatitude as well as stratosphere-troposphere exchange during Rossby wave breaking bringing in filaments of rich ozone airmass into the tropics. While massive airmass exchange, such as that due to Rossby wave breaking, can be captured by all instruments, there is a possibility whereby ozone filaments could be undetected by the satellite observations. Furthermore, different spectroscopic windows used by FTIR and other instruments used for this comparison might have also some contribution to the observed differences.

6 Conclusions

Ground-based FTIR spectrometry is a very useful technique to derive total column amounts and vertical profiles of many important trace gases in the atmosphere. This measurement site is located in a tropical region which is poorly constrained by ground-based instruments. As it provides unique information on the African continent, these measurements are of great importance for a better understanding of global climate and physical and chemical processes of the tropical atmosphere as well as for satellite validations.

A good agreement is determined from the intercomparison of O_3 profiles and column amounts from FTIR with that from the satellites instruments. The comparison of FTIR measurement of O_3 with that of MLS yields the mean relative differences of +11.0 to −18.8 % between 16.6 and 39.1 km, whereas comparison with MIPAS shows mean relative difference of ±18.4 % above 24.8 km. Similarly, comparison of FTIR with TES shows that the mean relative differences/absolute differences lie between −10.5 to +4.0 % (−0.6 ppmv to +0.3 ppmv) in the altitude range of 11.7–36.3 km. In general, minimum differences are observed at the region of peak ozone concentration. On the other hand, large differences are seen in the UTLS, which is partly explained by the effect of strong atmospheric gradients, since the UTLS regions oscillate back and forth with season and weather. The overall comparisons of column amounts of O_3 from satellite and the ground-based FTIR instruments show better agreement with mean relative differences within +0.2 % to +2.8 % and corresponding standard deviations of +2.0 % to +2.8 % for MLS and GOME-2; whereas, the mean relative differences are within a range of −0.9 to −9.0 % for intercomparison with OMI, TES, AIRS instruments.

The intercomparisons of O_3 VMR and column amounts from ground-based FTIR and several satellites reported in this work establish two major features that characterise both satellite and FTIR instruments. First, the good agreement between the O_3 VMRs and column amounts from FTIR with corresponding observations from satellites builds confidence in the FTIR observations. Second, though the satellite observations are already validated elsewhere, this is the first time observations of ozone from these instruments are compared with ground-based FTIR observations over tropical Africa. As a result, the observed agreement between the FTIR ozone observations with that of satellite observations builds also confidence in the validity of satellite observations over this particular region. Furthermore, the results of this intercomparison of FTIR observations with the satellites can ensure that FTIR observations can now be used to validate existing and future satellite missions.

Acknowledgements. We are grateful to the Goddard Space Flight Centre for providing temperature and pressure profiles via automailer system. We greatly acknowledge the MLS, MIPAS, TES, OMI, AIRS, and GOME science teams for the satellite data used in this study. We acknowledge support by Deutsche Forschungsgemeinschaft and Open Access Publishing Fund of Karlsruhe Institute of Technology. Finally, the author would like to thank Samara University for the sponsorship.

Edited by: J. Notholt

References

Balis, D., Kroon, M., Koukouli, M. E., Brinksma, E. J., Labow, G., Veefkind, J. P., and McPeters, R. D.: Validation of Ozone Monitoring Instrument total ozone column measurements using Brewer and Dobson spectrophotometer ground-based observations, J. Geophys. Res., 112, D24S46, doi:10.1029/2007JD008796, 2007.

Balis, D., Koukouli, M., Loyola, D., Valks, P., and Hao, N.: Second validation report of GOME-2 total ozone products (OTO/O_3, NTO/O_3) processed with GDP4.2, Report of the Satellite Application Facility on Ozone and Atmospheric Chemistry Monitoring (O3M-SAF), SAF/O3M/AUTH/GOME-2VAL/RP/02, 2008.

Barret, B., De Mazière, M., and Demoulin, P.: Retrieval and characterisation of ozone profiles from solar infrared spectra at the Jungfraujoch, J. Geophys. Res., 107, 4788, doi:10.1029/2001JD001298, 2002.

Barret, B., De Mazière, M., and Demoulin, P.: Correction to "Retrieval and characterisation of ozone profiles from solar infrared spectra at the Jungfraujoch", J. Geophys. Res., 108, 4372, doi:10.1029/2003JD003809, 2003.

Beer, R., Glavich, T., and Rider, D.: Tropospheric Emission Spectrometer for the Earth Observing System's Aura satellite, Appl. Opt., 40, 2356–2367, 2001.

Fischer, H., Birk, M., Blom, C., Carli, B., Carlotti, M., von Clarmann, T., Delbouille, L., Dudhia, A., Ehhalt, D., Endemann, M., Flaud, J. M., Gessner, R., Kleinert, A., Koopman, R., Langen, J., López-Puertas, M., Mosner, P., Nett, H., Oelhaf, H., Perron, G.,

Remedios, J., Ridolfi, M., Stiller, G., and Zander, R.: MIPAS: an instrument for atmospheric and climate research, Atmos. Chem. Phys., 8, 2151–2188, doi:10.5194/acp-8-2151-2008, 2008.

Fishman, J., John, K., Creilson, K. J., Wozniak, E. A., and Crutzen, J. P.: Interannual variability of stratospheric and tropospheric ozone determined from satellite measurements, J. Geophys. Res., 110, D20306, doi:10.1029/2005JD005868, 2005.

Froidevaux, L., Jiang, Y. B., Lambert, A., Livesey, N. J., Read, W. G., Waters, J. W., Browell, E. V., Hair, J. W., Avery, M. A., McGee, T. J., Twigg, L. W., Sumnicht, G. K., Jucks, K. W., Margitan, J. J., Sen, B., Stachnik, R. A., Toon, G. C., Bernath, P. F., Boone, C. D., Walker, K. A., Filipiak, M. J., Harwood, R. S., Fuller, R. A., Manney, G. L., Schwartz, M. J., Daffer, W. H., Drouin, B. J., Cofield, R. E., Cuddy, D. T., Jarnot, R. F., Knosp, B. W., Perun, V. S., Snyder, W. V., Stek, P. C., Thurstans, R. P., and Wagner, P. A.: Validation of Aura Microwave Limb Sounder stratospheric ozone measurements, J. Geophys. Res., 113, D15S20, doi:10.1029/2007JD008771, 2008.

Funke, B. and von Clarmann, T.: How to average logarithmic retrievals?, Atmos. Meas. Tech., 5, 831–841, doi:10.5194/amt-5-831-2012, 2012.

Griesfeller, A., Griesfeller, J., Hase, F., Krammer, I., Loes, P., Mikuteit, S., Raffalski, U., Blumentstock, T., and Nakajima, H.: Comparison of ILAS-II and ground-based FTIR measurements of O_3, HNO_3, N_2, and CH_4 over Kiruna, Sweden, J. Geophys. Res., 111, D11S07, doi:10.1029/2005JD006451, 2006.

Hase, F., Blumenstock, T., and Paton-Walsh, C.: Analysis of the instrumental line shape of high-resolution Fourier transform IR spectrometers with gas cell measurements and new retrieval software, Appl. Opt., 38, 3417–3422, 1999.

Hase, F., Hannigan, J. W., Coffey, M. T., Goldman, A., Hopfner, M., Jones, N. B., Rinsland, C. P., and Wood, S. W.: Intercomparison of retrieval codes used for the analysis of high-resolution, ground-based FTIR measurements, J. Quant. Spectrosc. Radiat. Transfer, 87, 25–52, 2004.

Hoogen, R., Rozanov, V. V., and Burrows, J. P.: Ozone profiles from GOME satellite data: Algorithm description and first validation, J. Geophys. Res., 104, 8263–8280, 1999.

Jarnot, R. F., Perun, V. S., and Schwartz, M. J.: Radiometric and spectral performance and calibration of the GHz bands of EOS MLS, IEEE Trans. Geosci. Remote Sens., 44, 1131–1143, doi:10.1109/TGRS.2005.863714, 2006.

Jiang, Y. B., Froidevaux, L., Lambert, A., Livesey, N. J., Read, W. G., Waters, J. W., Bojkov, B., Leblanc, T., McDermid, I. S., Godin-Beekmann, S., Filipiak, M. J., Harwood, R. S., Fuller, R. A., Daffer, W. H., Drouin, B. J., Cofield, R. E., Cuddy, D. T., Jarnot, R. F., Knosp, B. W., Perun, V. S., Schwartz, M. J., Snyder, W. V., Stek, P. C., Thurstans, R. P., Wagner, P. A., Allaart, M., Andersen, S. B., Bodeker, G., Calpini, B., Claude, H., Coetzee, G., Davies, J., De Backer, H., Dier, H., Fujiwara, M., Johnson, B., Kelder, H., Leme, N. P., König-Langlo, G., Kyro, E., Laneve, G., Fook, L. S., Merrill, J., Morris, G., Newchurch, M., Oltmans, S., Parrondos, M. C., Posny, F., Schmidlin, F., Skrivankova, P., Stubi, R., Tarasick, D., Thompson, A., Thouret, V., Viatte, P., Vomel, H., von Der Gathen, P., Yela, M., and Zablocki, G.: Validation of Aura Microwave Limb Sounder Ozone by ozonesonde and lidar measurements, J. Geophys. Res., 112, D24S34, doi:10.1029/2007JD008776, 2007.

Holton, J. R.: Introduction to dynamic meteorology, forth edition, Department of Atmospheric Science University of Washington, Elsevier Academic Press, 2004.

Jacobson, M. Z.: Fundamentals of Atmospheric Modeling, 2nd Edn., Stanford University, Cambridge University press, 2005.

Levelt, P. F., van den Oord, G. H. J., Dobber, M. R., Malkki, A., Visser, H., de Vries, J., Stammes, P., Lundell, J. O. V., and Saari, H.: The Ozone Monitoring Instrument, IEEE T. Geosci. Remote, 44, 1093–1101, 2006.

Lindenmaier, R., Batchelor, R. L., Strong, K., Fast, H., Goutail, F., Kolonjari, F., McElroy, C. T, Mittermeier, R. L., and Walker, K. A.: An evaluation of infrared microwindows for ozone retrievals using the Eureka Bruker 125HR Fourier transform spectrometer, J. Quant. Spectrosc. Radiat. Transfer, 111, 569–585, 2010.

Livesey, N. J., Filipiak, M. J., Froidevaux, L., Read, W. G., Lambert, A., Santee, M. L., Jiang, J. H., Pumphrey, H. C., Waters, J. W., Cofield, R. E., Cuddy, D. T., Daffer, W. H., Drouin, B. J., Fuller, R. A., Jarnot, R. F., Jiang, Y. B., Knosp, B. W., Li, Q. B., Perun, V. S., Schwartz, M. J., Snyder, W. V., Stek, P. C., Thurstans, R. P., Wagner, P. A., Avery, M., Browell, E. V., Cammas, J. P., Christensen, L. E., Diskin, G. S., Gao, R. S., Jost, H. J., Loewenstein, M., Lopez, J. D., Nedelec, P., Osterman, G. B., Sachse, G. W., and Webster, C. R.: Validation of Aura Microwave Limb Sounder O_3 and CO observations in the upper troposphere and lower stratosphere, J. Geophys. Res., 113, D15S02, doi:10.1029/2007JD008805, 2008.

Lucke, R. L., Korwan, D., Bevilacqua, R. M., Hornstein, J. S., Shettle, E. P., Chen, D. T., Daehler, M., Lumpe, J. D., Fromm, M. D., Debrestian, D., Neff, B., Squire, M., Konig-Langlo, G., and Davies, J.: The Polar Ozone and Aerosol Measurement (POAM III) Instrument and Early Validation Results, J. Geophys. Res., 104, 18785–18799, 1999.

Mengistu Tsidu, G.: The role of chemistry and transport on NO_y partitioning and budget during Austral Spring 2002 as derived from MIPAS measurement, PhD dissertation, institute für meteorologie and Klimaforschung, Germany, 2005.

Mengistu Tsidu, G.: High resolution monthly rainfall database for Ethiopia: Homogenization, Reconstruction, and Gridding, J. Climate, 25, 8422–8443, doi:10.1175/JCLI-D-12-00027.1, 2012.

Mengistu Tsidu, G. and Ture, K.: Mechanisms of ozone enhancement during stratospheric intrusion coupled with convection over upper troposphee equatorial Africa, Atmos. Environ., doi:10.1016/j.atmosenv.2013.01.024, in press, 2013.

Nassar, R., Logan, J. A., Worden, H. M., Megretskaia, I. A., Bowman, K. W., Osterman, G. B., Thompson, A. M., Tarasick, D. W., Austin, S., Claude, H., Dubey, M. K., Hocking, W. K., Johnson, B. J., Joseph, E., Merrill, J., Morris, G. A., Newchurch, M., Oltmans, S. J., Posny, F., Schmidlin, F. J., Vömel, H., Whiteman, D. N., and Witte, J. C.: Validation of Tropospheric Emission Spectrometre (TES) nadir ozone profiles using ozonesonde measurements, J. Geophys. Res., 113, D15S17, doi:10.1029/2007JD008819, 2008.

Notholt, J., Toon, G., Jones, N., Griffith, D., and Warneke, T.: Spectral line finding program for atmospheric remote sensing using full radiation transfer, J. Quant. Spectrosc. Radiat. Transfer, 97, 112–125, doi:10.1016/j.jqsrt.2004.12.025, 2004.

Petersen, A. K.: Atmospheric Trace Gas Measurements in the Tropics, PhD dissertation, University at Bremen Fachbereich fur Physik und Elektrotechnik Institut fur Umweltphysik, Germany,

2009.

Petersen, A. K., Warneke, T., Lawrence, M. G., Notholt, J., and Schrems, O.: First ground-based FTIR observations of the seasonal variation of carbon monoxide in the tropics, Geophys. Res. Lett., 35, L03813, doi:10.1029/2007GL031393, 2008.

Petersen, A. K., Warneke, T., Frankenberg, C., Bergamaschi, P., Gerbig, C., Notholt, J., Buchwitz, M., Schneising, O., and Schrems, O.: First ground-based FTIR observations of methane in the inner tropics over several years, Atmos. Chem. Phys., 10, 7231–7239, doi:10.5194/acp-10-7231-2010, 2010.

Phillips, D.: A technique for the numerical solution of certain integral equations of first kind, J. Assoc. Comput. March, 9, 84–97, 1962.

Richards, N., Osterman, G. B., Browell, E. V., Hair, J., Avery, A., and Li, Q. B.: Validation of Tropospheric Emission Spectrometre (TES) ozone profiles with aircraft observations during INTEX-B, J. Geophys. Res., 113, D16S29, doi:10.1029/2007JD008815, 2008.

Rinsland, C. P., Goldman, A., Murcray, F. J., Murcray, F. H., Blatherwick, R. D., and Murcray, D. G.: Infrared Measurements of Atmospheric Gases Above Mauna Loa, Hawaii, in February 1987, J. Geophys. Res., 93, 12607–12626, doi:10.1029/JD093iD10p12607, 1988.

Rodgers, C. D.: Retrieval of atmospheric temperature and composition from remote measurements of thermal radiation, Rev. Geophys., 14, 609–624, 1976.

Rodgers, C. D.: Inverse Methods for Atmospheric Sounding Theory and Practise, in: Series on Atmospheric, Oceanic and Planetary Physics, World Scientific (publisher), Vol. 2, 2000.

Rodgers, C. D. and Connor, B. J.: Intercomparison of remote sounding instruments, J. Geophys. Res., 108, 4116–4130, doi:10.1029/2002JD002299, 2003.

Rothman, L. S., Jacquemart, D., Barbe, A., Chris Bennerc, D., Birk, M., Brown, L. R., Carleer, M. R., Chackerian Jr., C., Chance, K., Coudert, L. H., Dana, V., Devi, V .M., Flaud, J. M., Gamache, R. R., Goldman, A., Hartmann, J. M., Jucks, K.W., Maki, A. G., Mandin, J. Y., Massie, S. T., Orphal, J., Perrin, A., Rinsland, C. P., Smith, M. A. H., Tennyson, J., Tolchenov, R. N., Toth, R. A., Vander Auwera, J., Varanasi, P., and Wagner, G.: The HITRAN 2004 molecular spectroscopic database, J. Quant. Spectrosc. Radiat. Transfer, 96, 139–204, 2005.

Schneider, M.: Continuous observations of atmospheric trace gases by ground-based FTIR spectroscopy at Izana observatory, Tenerife Island, PhD dissertation, at institute of Metrology and Klimaforschung, 2002.

Schneider, M., Blumenstock, T., Hase, F., Höpfner, M, Cuevas, E., Redondas, A., and Sancho, J. M.: Ozone profiles and total column amounts drived at Izaña, Tenerife Island, from FTIR solar absorption spectra, and its validation by intercomparision to ECC-sonde and Brewer spectrometer measurements, J. Quant. Spectrosc. Radiat. Transfer, 91, 245–274, 2005a.

Schneider, M., Hase, F., and Blumenstock, T.: Water vapour profiles by ground-based FTIR spectroscopy: study for an optimised retrieval and its validation, Atmos. Chem. Phys., 6, 811–830, doi:10.5194/acp-6-811-2006, 2006a.

Schneider, M., Hase, F., Blumenstock, T., Redondas, A., and Cuevas, E.: Quality assessment of O_3 profiles measured by a state-of-the-art ground-based FTIR observing system, Atmos. Chem. Phys., 8, 5579–5588, doi:10.5194/acp-8-5579-2008, 2008.

Schoeberl, M. R., Douglass, A. R., Hilsenrath, E., Bhartia, P. K., Beer, R., Waters, J. W., Gunson, M. R., Froidevaux, L., Gille, J. C., Barnett, J. J., Levelt, P. F., and DeCola, P.: Overview of the EOS Aura mission, IEEE Trans. Geosci. Remote Sens., 44, 1066–1074, 2006.

Senten, C., De Mazière, M., Dils, B., Hermans, C., Kruglanski, M., Neefs, E., Scolas, F., Vandaele, A. C., Vanhaelewyn, G., Vigouroux, C., Carleer, M., Coheur, P. F., Fally, S., Barret, B., Baray, J. L., Delmas, R., Leveau, J., Metzger, J. M., Mahieu, E., Boone, C., Walker, K. A., Bernath, P. F., and Strong, K.: Technical Note: New ground-based FTIR measurements at Ile de La Réunion: observations, error analysis, and comparisons with independent data, Atmos. Chem. Phys., 8, 3483–3508, doi:10.5194/acp-8-3483-2008, 2008.

Steck, T., von Clarmann, T., Fischer, H., Funke, B., Glatthor, N., Grabowski, U., Höpfner, M., Kellmann, S., Kiefer, M., Linden, A., Milz, M., Stiller, G. P., Wang, D. Y., Allaart, M., Blumenstock, Th., von der Gathen, P., Hansen, G., Hase, F., Hochschild, G., Kopp, G., Kyrö, E., Oelhaf, H., Raffalski, U., Redondas Marrero, A., Remsberg, E., Russell III, J., Stebel, K., Steinbrecht, W., Wetzel, G., Yela, M., and Zhang, G.: Bias determination and precision validation of ozone profiles from MIPAS-Envisat retrieved with the IMK-IAA processor, Atmos. Chem. Phys., 7, 3639–3662, doi:10.5194/acp-7-3639-2007, 2007.

Stiller, G. P., Kiefer, M., Eckert, E., von Clarmann, T., Kellmann, S., García-Comas, M., Funke, B., Leblanc, T., Fetzer, E., Froidevaux, L., Gomez, M., Hall, E., Hurst, D., Jordan, A., Kämpfer, N., Lambert, A., McDermid, I. S., McGee, T., Miloshevich, L., Nedoluha, G., Read, W., Schneider, M., Schwartz, M., Straub, C., Toon, G., Twigg, L. W., Walker, K., and Whiteman, D. N.: Validation of MIPAS IMK/IAA temperature, water vapour, and ozone profiles with MOHAVE-2009 campaign measurements, Atmos. Meas. Tech., 5, 289–320, doi:10.5194/amt-5-289-2012, 2012.

Tikhonov, A.: On the solution of incorrectly stated problems and method of regularization, Dokl. Akad, Nauk. SSSR, 151, 501–504, 1963.

Van Roozendael, M., Lambert, J. C., Spurr, R. J. D., and Fayt, C.: GOME Direct Fitting (GODFIT) GDOAS Delta Validation Report, ERS Exploitation AO/1-4235/02/I-LG, Oberpfaffenhofen, Germany, 2004.

Viatte, C., Schneider, M., Redondas, A., Hase, F., Eremenko, M., Chelin, P., Flaud, J.-M., Blumenstock, T., and Orphal, J.: Comparison of ground-based FTIR and Brewer O_3 total column with data from two different IASI algorithms and from OMI and GOME-2 satellite instruments, Atmos. Meas. Tech., 4, 535–546, doi:10.5194/amt-4-535-2011, 2011.

Vigouroux, C., De Mazière, M., Errera, Q., Chabrillat, S., Mahieu, E., Duchatelet, P., Wood, S., Smale, D., Mikuteit, S., Blumenstock, T., Hase, F., and Jones, N.: Comparisons between ground-based FTIR and MIPAS N_2O and HNO_3 profiles before and after assimilation in BASCOE, Atmos. Chem. Phys., 7, 377–396, doi:10.5194/acp-7-377-2007, 2007.

von Clarmann, T., Höpfner, M., Kellmann, S., Linden, A., Chauhan, S., Funke, B., Grabowski, U., Glatthor, N., Kiefer, M., Schieferdecker, T., Stiller, G. P., and Versick, S.: Retrieval of temperature, H_2O, O_3, HNO_3, CH_4, N_2O, $ClONO_2$ and ClO from MIPAS reduced resolution nominal mode limb emission measurements,

Atmos. Meas. Tech., 2, 159–175, doi:10.5194/amt-2-159-2009, 2009.

Worden, H. M., Logan, J. A., Worden, J. R., Beer, R., Bowman, K., Clough, S. A., Eldering, A., Fisher, B. M., Gunson, M. R., Herman, R. L., Kulawik, S. S., Lampel, M. C., Luo, M., Megretskaia, I. A., Osterman, G. B., and Shephard, M. W.: Comparisons of Tropospheric Emission Spectrometer (TES) ozone profiles to ozonesondes: Methods and initial results, J. Geophys. Res., 112, D03309, doi:10.1029/2006JD007258, 2007.

Wunch, D., Taylor, J. R., Fu, D., Bernath, P., Drummond, J. R., Midwinter, C., Strong, K., and Walker, K. A.: Simultaneous ground-based observations of O_3, HCl, N_2O, and CH_4 over Toronto, Canada by three Fourier transform spectrometers with different resolutions, Atmos. Chem. Phys., 7, 1275–1292, doi:10.5194/acp-7-1275-2007, 2007.

Won, Y.-I.: Document for AIRS Level-3 Version 5 Standard Products, GES DISC, 3 March, 2008.

Zhang, L., Jacob, D. J., Liu, X., Logan, J. A., Chance, K., Eldering, A., and Bojkov, B. R.: Intercomparison methods for satellite measurements of atmospheric composition: application to tropospheric ozone from TES and OMI, Atmos. Chem. Phys., 10, 4725–4739, doi:10.5194/acp-10-4725-2010, 2010.